ELSEVIER

Ceramics International 33 (2007) 537–542

CERAMICS INTERNATIONAL

www.elsevier.com/locate/ceramint

# Preparation of nanosized tin oxide ($SnO_2$) powder by homogeneous precipitation

Özge Acarbaş [a], Ender Suvacı [a,b,*], Aydın Doğan [a]

[a] *Anadolu University, Department of Materials Science and Engineering, Iki Eylul Campus, 26480 Eskisehir, Turkey*
[b] *TUBITAK-Ceramic Research Centre, Anadolu University 26480 Eskisehir, Turkey*

Received 24 March 2005; received in revised form 5 September 2005; accepted 6 October 2005
Available online 3 February 2006

**Abstract**

Synthesis of nanosized $SnO_2$ ceramic particles via homogeneous precipitation was investigated as a function of processing parameters such as initial concentration and calcination temperature. Hydrous tin oxide was precipitated from 0.01 to 1 M $SnCl_4$-urea aqueous solutions by decomposition of urea at ~90 °C. Initial concentration has a significant effect on phase formation and crystallite size of the prepared powder. The crystallite size of tin dioxide increased with increasing initial concentration. For example, while crystallite size was 11.7 nm for 0.033 M $SnCl_4$ system, it was 25.3 nm for 0.25 M $SnCl_4$ system. In addition, tin dioxide particles as small as a few nanometers were obtained by homogeneous precipitation. However, calcination resulted in crystal growth and agglomeration and subsequently, reduction in the effective surface area of tin dioxide powders.


*Keywords:* Homogeneous precipitation; Tin dioxide; Nanosized ceramic particles

## 1. Introduction

Tin dioxide ($SnO_2$) is an important semiconducting material which has been widely used in an extensive range of applications such as catalysts [1,2], gas sensors [3,4], heat mirrors [5,6], varistors [7,8], transparent electrodes for solar cells [9,10], glass melting electrodes and optoelectronic devices [11]. Tin dioxide-based gas sensors are very important n-type semiconductor sensors which can be utilized to detect various inflammable and harmful gases such as hydrogen ($H_2$) and carbon monoxide (CO).

Semiconductor sensors exhibit changes in electrical resistivity in the presence of small concentrations of certain gases. The sensing behavior of n-type semiconductors is controlled by the adsorption of oxygen on the surface of metal oxides. As adsorption proceeds a positive space charge develops in the oxide as electrons transfer from the conduction band or from donor dopants to the adsorbed oxygen, and a corresponding negative charge (i.e., $O_2^-$, $O^-$ and $O^{2-}$) accumulates on the surface. Therefore, the resistivity of an n-type semiconductor gas sensor in air is high due to the development of a potential barrier to electronic conduction at each grain boundary. When the sensor is exposed to an atmosphere containing reducing gases, the oxygen adsorbates are consumed and a decrease in the resistivity occurs due to the decrease in the potential barrier for conduction [3,4]. Sensors consisting of fine particles of metal oxides usually exhibit high sensitivity. Accordingly, one of the most important factors affecting sensitivity of the sensors is the actual grain or crystallite size of the sensor materials and subsequently space-charge depth. Consequently, semiconductor sensors should be composed of fine crystallites to achieve high sensitivities [4].

The tin dioxide used for gas sensors has been synthesized by various synthesis methods such as direct strike precipitation [12,13], two-step solid state synthesis [14], microemulsion [15], sol–gel [16], spray pyrolysis [17], gel combustion technique (i.e., Pechini method) [18], hydrothermal synthesis [19]. Among these methods conventionally accepted method is the synthesis of tin dioxide particles from precursor hydroxides precipitated by the direct addition of $NH_4OH$ to $SnCl_4$ aqueous solutions. Although, this technique yields a large amount of powder at once and at a reasonable cost, it is not easy to obtain high surface area powders because of the irregular particle

* Corresponding author. Tel.: +90 222 3213550x6386; fax: +90 222 3239501.
*E-mail addresses:* esuvaci@anadolu.edu.tr, esuvaci@yahoo.com (E. Suvacı).

0272-8842/$32.00 
doi:10.1016/j.ceramint.2005.10.024

morphology, large particle size distribution and the high degree of agglomeration [12,13]. Those problems arise due to the nonuniform supersaturation in solution. If uniform supersaturation is achieved in solution then physical powder characteristics can be controlled precisely. Controlled precipitation is best accomplished via homogeneous precipitation which utilizes chemical reactions (e.g., urea decomposition) whose kinetics rate limit the release of supersaturating species [20–22]. Homogeneous precipitation method, using urea as a reagent to control the pH and to obtain a pure and dense hydrous tin oxide precipitates, was investigated earlier by Gordon [23] and recently by Song and Kang [12]. The former study focused on formation of hydrous tin oxide via homogeneous precipitation under various conditions, instead of tin dioxide formation. In the latter study, tin dioxide powders were synthesized by both homogeneous precipitation and direct precipitation from $SnCl_4$ solutions. The powders from homogeneous method had higher surface areas (24–44 $m^2/g$) than those of the direct precipitated powders (15–18 $m^2/g$). Since the study focused mainly on the comparison of powders produced by two methods; the processing details were discussed briefly in that paper. Therefore, the research objectives of this study were to investigate the processing parameter effects (initial concentration and calcination temperature) on particle characteristics and to understand the particle formation steps during the synthesis of tin dioxide via homogeneous precipitation.

## 2. Experimental procedure

In this study, 0.01–2 M aqueous solutions of tin tetrachloride ($SnCl_4$) and urea ($(NH_2)_2CO$) were utilized as starting materials. Feedstock solutions for synthesis were prepared by mixing urea and tin tetrachloride solutions at a ratio of 2:1. Table 1 summarizes the solution systems studied in this work. Unless otherwise noted, all concentrations reported in the paper refer to feedstock solution concentrations. The feedstock solution was heated to 90 °C and held there for 90 min to complete the synthesis process while it was being stirred [24]. Solution pH was monitored before and after the synthesis. After the synthesis, solutions were washed with distilled water five times in a centrifuge and after each washing step, conductivity of supernatant was measured by a conductivity meter to make sure efficient removal of ions from solutions. Then, precipitates were dried at 90 °C for 24–72 h in a drying oven. After drying, unless otherwise noted, all samples were calcined at 800 °C for 2 h. Fig. 1 shows the process flow chart used to synthesize nanosized tin dioxide particles by homogeneous precipitation in this study.

Table 1
Summary of the solution systems utilized in this study

| Sample | Molarity before mixing | | Molarity in feedstock solution | | Remarks |
|---|---|---|---|---|---|
| | $SnCl_4$ | Urea | $SnCl_4$ | Urea | |
| A | 0.01 | 0.01 | $3.33 \times 10^{-3}$ | $6.66 \times 10^{-3}$ | Precipitation |
| B | 0.1 | 0.1 | 0.033 | 0.067 | Precipitation |
| C | 0.5 | 0.5 | 0.167 | 0.333 | Precipitation |
| D | 1 | 1 | 0.25 | 0.5 | Precipitation |
| E | 1.5 | 1.5 | 0.5 | 1 | No precipitation |
| F | 2 | 2 | 0.67 | 1.33 | No precipitation |

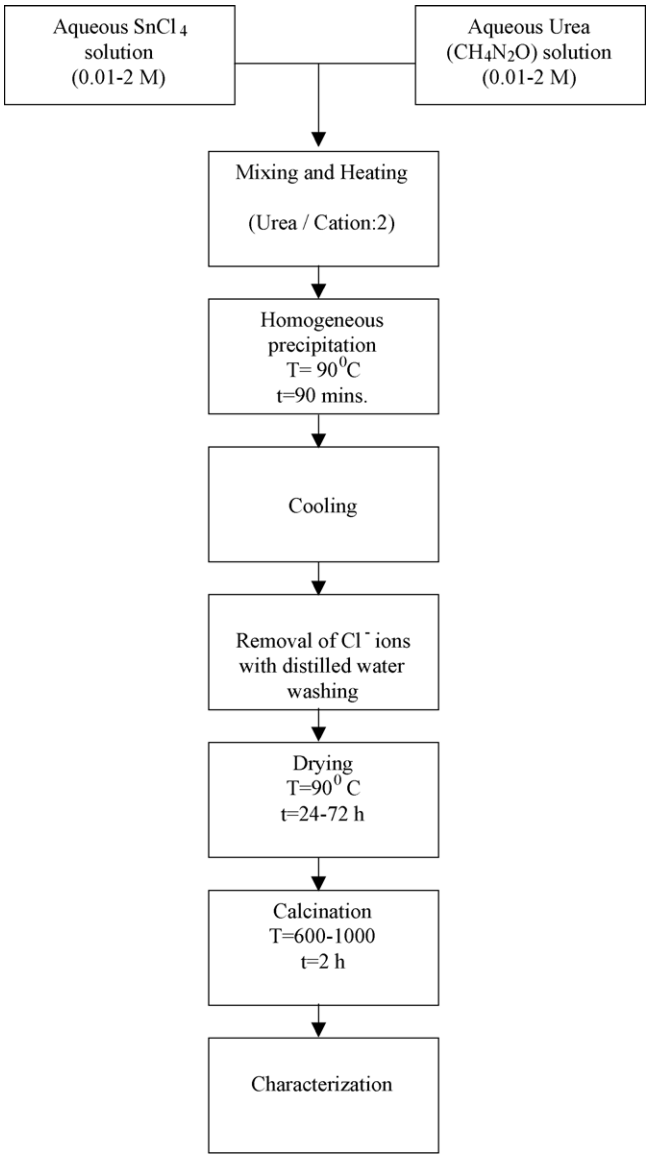


Fig. 1. The process flow chart used for synthesis of nanosized $SnO_2$ powders by homogeneous precipitation.

Phase development during the process was monitored by Fourier-transformed infrared spectroscopy (FTIR) and X-ray diffraction (XRD) techniques. Samples were diluted with KBr and pressed into a disk shape prior to FTIR analyses. XRD measurements were carried out between 20° and 70° with 2°/min. Thermochemical behavior of the precipitated phase was characterized by thermogravimetric (TGA) and differential thermal (DTA) analyzers. Morphological properties of the prepared powders were observed by field emission scanning electron microscope (FESEM). Specific surface areas of the powders were measured by a gas adsorption (Brunauer-Emmett-Teller, BET) technique. All samples were degassed at 150 °C for 2 h prior to BET analyses.

## 3. Results and discussion

### 3.1. Phase development

Precipitation from clear solutions of urea and tin tetrachloride mixtures was observed at $T > 80\ ^{\circ}C$ due to the decomposition of urea into $NH_3$ and $CO_2$. Fig. 2 shows the XRD pattern of the precipitated phase after washing and drying (i.e., uncalcined). Although the precipitated phase is mainly amorphous, broad peaks on the pattern suggest some degree of crystallinity in the precipitated phase. In addition, peak occurs at about 556 $cm^{-1}$ in the FTIR pattern (Fig. 3) also indicates formation of Sn–O terminal bonds during the precipitation [25]. Besides, peak at about 1618 $cm^{-1}$ shows presence of $H_2O$ in the precipitated phase [25]. The small peak at ~1399 $cm^{-1}$ is an indication for adsorbed carbonate species on the precipitate surface [25]. Both XRD and FTIR data of the precipitated phase indicate formation of hydrous tin oxide phase from the homogeneous precipitation. These results are consistent with the literature, which report formation of a hydrous tin oxide as a result of the precipitation from aqueous $SnCl_4$ solutions [21,26].

TGA and DTA analyses were performed to determine thermal behavior of the precipitated phase and hence to choose an optimum calcination temperature. Fig. 4a and b demonstrate TGA and DTA data, respectively, for the systems studied in this work. Total weight loss occurs in two stages as shown in TGA data: First, weight loss is observed at $T < \sim 150\ ^{\circ}C$ due to physically adsorbed water and this results in an endothermic peak in the DTA data (Fig. 4b).

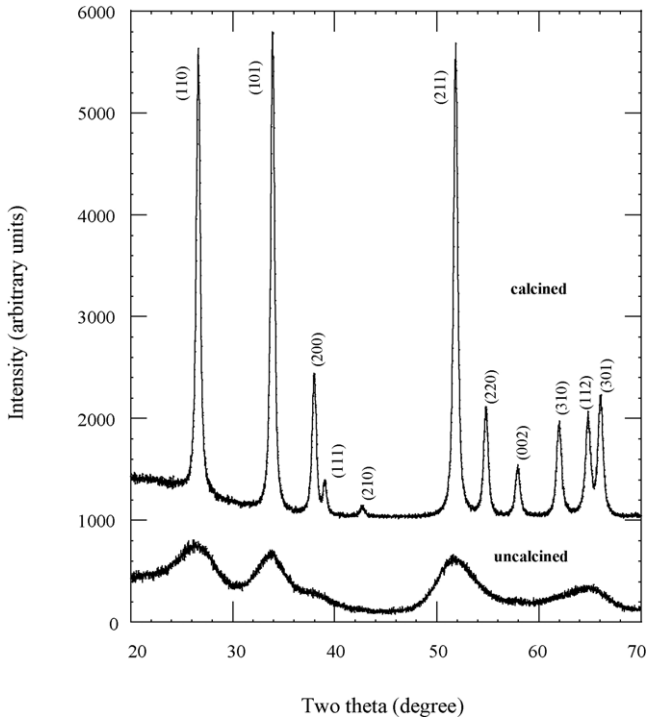


Fig. 2. The XRD patterns of sample C before and after calcination. Calcination condition was 800 °C, 2 h. Peaks were indexed according to JCPDS card of SnO2 (card no. 41–1445).

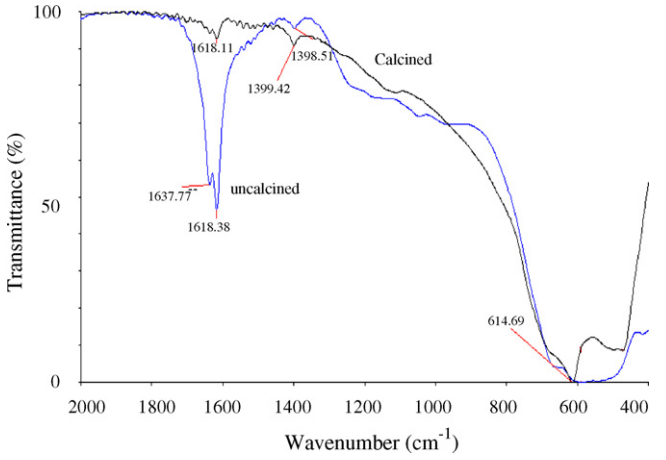


Fig. 3. The FTIR plots of sample C before and after calcination. (Calcination condition was 800 °C, 2 h).

Secondly, chemically adsorbed water is removed from the system at $T > 150\ ^{\circ}C$. Since the weight loss occurs gradually during that stage, the endothermic peak is not as apparent as that of the first stage. Although it has been reported by Song and Kang [12] previously for a similar system, no exothermic peak around 240 °C due to the decomposition of $NH_4^+$ was observed in this study. This difference may be attributed to adequate washing of the precipitated phase and, subsequently, efficient removal of $NH_4^+$ ions in this study. The results of TGA and DTA studies indicate that when the precipitated phases are heated at temperatures as low as 600 °C, all the reactions in the system are complete. That is, further heating (above 600 °C) of the precipitated phases does not cause any thermal and/or weight changes. The total weight losses are ~17, 16 and 15% for samples B, C and D, respectively. These values are also in agreement with the previous studies where 12–17% total weight losses were reported for aqueous $SnCl_4$-based systems [26].

FTIR data shows the removal of $H_2O$ peak at 1618 $cm^{-1}$ after calcination at 800 °C for 2 h (Fig. 3). In addition, switching from terminal Sn–O bonds (556 $cm^{-1}$) to bridging Sn–O bonds (615 $cm^{-1}$) (Fig. 3) suggests a crystallographic rearrangement in the precipitated phase during calcination [25]. Besides, the XRD data confirms crystallization and formation of crystalline $SnO_2$ powders from hydrous tin oxide after calcination at 800 °C for 2 h (Fig. 2). Since the prepared powder has a high surface area and subsequently high reactivity, small peaks at 1399 and 1618 $cm^{-1}$ are indication of presence of water and carbonate molecules which are adsorbed to the surface of tin dioxide powders during handling of the powder [25].

### 3.2. Effect of processing parameters on powder characteristics

#### 3.2.1. Initial concentration

In order to understand effect of initial concentration on homogeneous precipitation of tin dioxide ceramic particles, initial concentrations of urea and tin tetrachloride (in feedstock

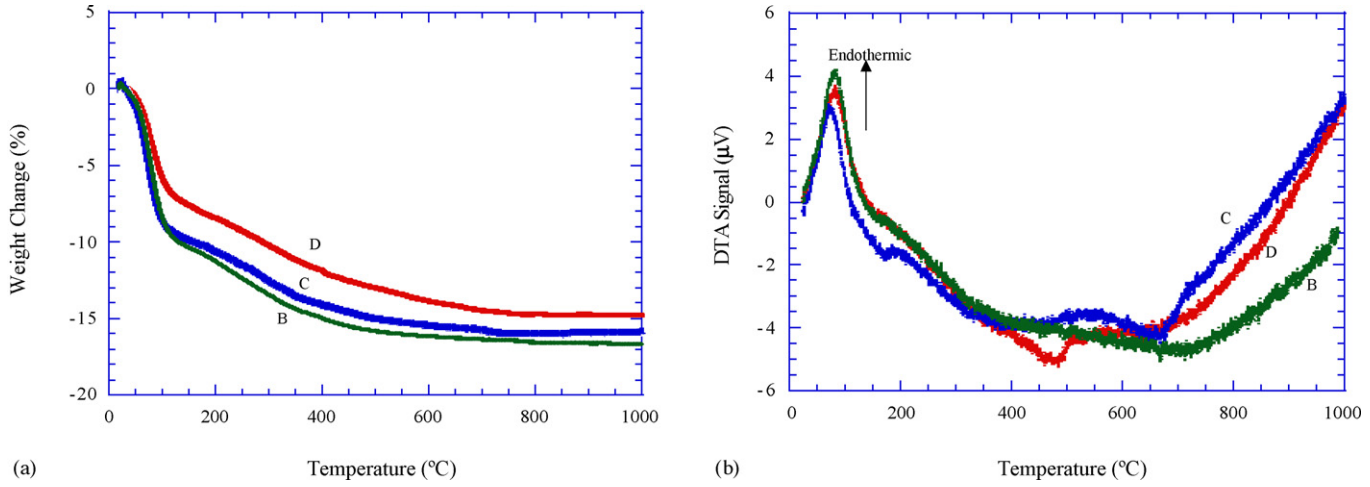


Fig. 4. (a) Effect of heating on weight change of the precipitated hydrous tin oxide powders in sample B, C and D (heating rate = 5 °/min). (b) DTA analyses of the samples B, C and D.

solutions) were varied from $6.7 \times 10^{-3}$ M to 1.33 M, and from $3.3 \times 10^{-3}$ M to 0.67 M, respectively, while the urea: tin tetrachloride ratio was constant as 2:1. Precipitation was observed in the systems containing less than 0.5 M $SnCl_4$; however, at high concentrations ($\geq$0.5 M $SnCl_4$) although the samples were aged overnight no precipitation was observed (Table 1). Fig. 5 demonstrates XRD patterns of the samples after calcination at 800 °C for 2 h. All samples exhibit single $SnO_2$ phase (in tetragonal rutile structure) with high crystallinity except sample A which shows lower degree of crystallinity.

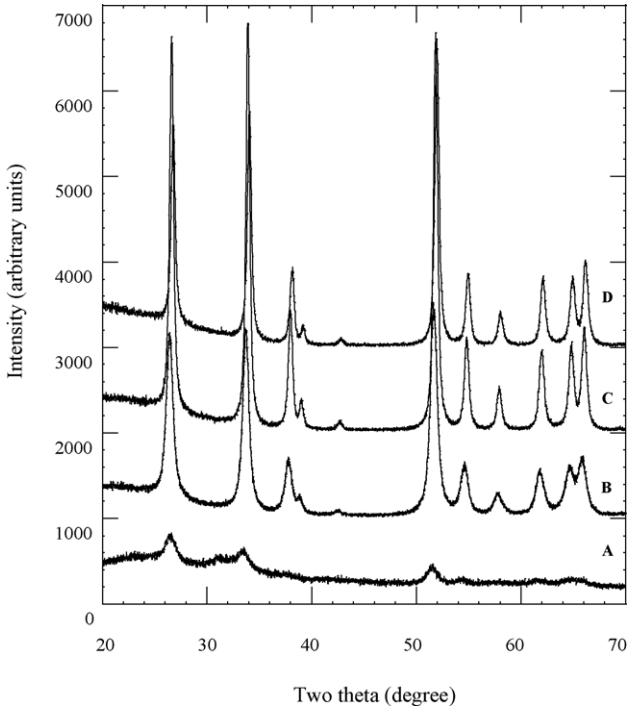


Fig. 5. The XRD patterns of samples A, B, C and D (All samples were calcined at 800 °C, 2 h).

The crystallite sizes of produced tin dioxide samples were calculated by means of X-ray line broadening measurement according to Scherrer equation [26]:

$$D = \frac{0.9\lambda}{\beta \cos\theta} \quad (1)$$

where $D$, mean crystallite size, $\lambda$, wavelength (i.e., 1.5418 Å for Cu K$\alpha$), $\beta$, full width half maximum of $SnO_2$ (1 1 0) line after instrumental broadening effects are eliminated [27] and $2\theta$, diffraction angle for the (1 1 0) line (in radian). Table 2 shows the effect of initial concentration on crystallite size of tin dioxide powders. The crystallite size increases with increasing initial concentration. For example, while crystallite size is 11.7 nm for 0.033 M $SnCl_4$ system, it is 19.8 and 25.3 nm for 0.17 and 0.25 M $SnCl_4$ systems, respectively. SEM micrographs of samples B and C also confirm increase in crystallite size with increasing initial concentration (Fig. 6). These results can be attributed one of the following reasons: The first possible scenario is that higher concentration might have resulted in finer particles during synthesis as predicted by classical nucleation theory, which would predict higher supersaturation conditions and smaller crystals at higher initial concentrations [28]. Meanwhile, the calcination step results in partial sintering and subsequent grain growth. Since finer particles sinter faster than coarser ones, initially finer particles may have longer time for the growth. Accordingly, the particle size of the tin oxide particles could have predicted as increasing with increasing initial concentration due to the grain growth during the calcina-

Table 2
Effect of initial concentration on crystallite size of tin oxide ceramic particles. (Samples were calcined at 800 °C, 2 h)

| Initial $SnCl_4$ concentration in feedstock solution | Crystallite size (nm) |
|---|---|
| 0.0033 | 7.7 |
| 0.033 | 11.7 |
| 0.167 | 19.8 |
| 0.25 | 25.3 |

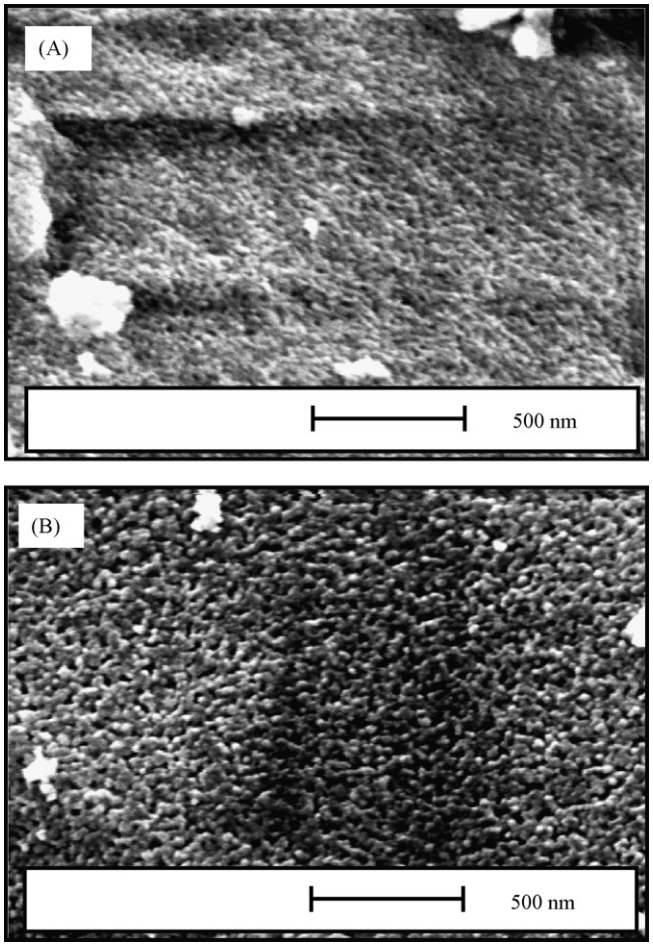


Fig. 6. SEM micrographs of samples (a) B and (b) C (samples were calcined at 800 °C, 2 h).

tion. Another possibility is that although these results are not supported by classical nucleation and growth model, they may be resulted by continuous generation of reacting species throughout the particle formation process. That is, high initial concentration (i.e., high initial supersaturation) results in a large number of nuclei with very small crystallite size and some of those nuclei (''unstable nuclei'') dissolve and reprecipitate on undissolved, ''stable'', nuclei (i.e., growth of crystals) to maintain the supersaturation during the particle formation process. Thus, some particles grow at the expense of others. This type of particle formation behavior has already been observed in some systems [29,30]. Furthermore, close examination of the TGA analyses (Fig. 4a) reveals that as the initial concentration increased total weight loss decreases. This result can be attributed to increasing surface area (i.e., decreasing particle size) with decreasing initial concentration during the synthesis. This suggested mechanism may also explain why precipitation was not observed in highly concentrated samples. Large number of unstable nuclei formation may have resulted limited or no precipitation at high concentrations in this study. However, a more detailed research should be conducted to test these hypotheses. These results show that initial concentration has significant effect on the particle size and the phase formation during the tin dioxide powder synthesis via homogeneous precipitation.

### 3.2.2. Calcination temperature

Fig. 7 shows the XRD patterns of sample D as a function of calcination temperature. The patterns show that even after heating at 600 °C for 2 h, the sample exhibits high degree of crystallinity and this pattern does not change much with increasing temperature. Table 3 shows dependence of crystallite size of sample D to calcination temperature. As the temperature increases, size of tin dioxide crystals increases. For example, while the crystallite size of the sample, calcined at 600 °C for 2 h, is 10.8 nm, the sample exhibits 25.3 and 35.9 nm crystallite size after calcination at 800 and 1000 °C, respectively, for 2 h. These results confirm crystal growth during the process of calcination. In addition, comparison of equivalent spherical diameter, esd, values (obtained from BET results) with crystallite sizes (obtained from XRD data) reveals possible agglomeration during the calcination. For example, while the crystallite size of the 1 M sample increases from 10.8 to 25.3 nm after switching the calcination temperature from 600 to 800 °C, equivalent spherical diameters are 35 (specific surface area: 25 $m^2$/g) and 110 nm (specific surface area: 8 $m^2$/g), respectively. That is, agglomerates at 800 °C are formed by more number of crystals with respect to 600 °C. Fig. 6 also shows the agglomerated nature of the tin dioxide particles after the calcination. Thus, the calcination results not only in crystal growth but also in agglomeration of homogeneously precipitated tin dioxide powders. Accordingly, specific surface area of tin dioxide particles decreases with increasing the calcination temperature. For example, specific surface area of uncalcined sample B powder is about 173 $m^2$/g (esd: 5 nm) whereas when the same sample is calcined at 600 and 800 °C for 2 h, the specific surface area of the powder becomes 21.5 (esd: 40.8 nm) and 10.4 $m^2$/g (esd: 84.4 nm), respectively. These results show that tin dioxide particles as small as a few nanometers can be precipitated by homogeneous precipitation.

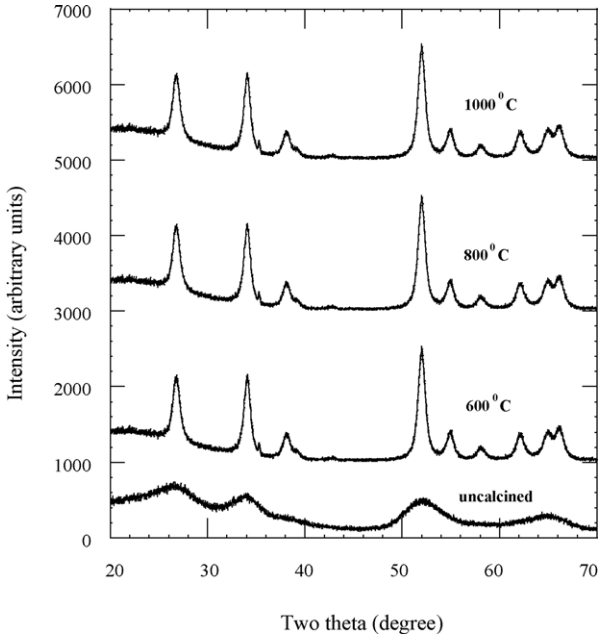


Fig. 7. The XRD patterns of sample D before and after calcination at 600, 800 and 1000 °C, 2 h.

Table 3
Effect of calcination temprerature on crystallite size. (Calcination time was 2 h for all samples)

| Calcination temperature (°C) | Crystallite size (nm) |
|---|---|
| 600 | 10.8 |
| 800 | 25.3 |
| 1000 | 35.9 |

Unfortunately, calcination process results in crystal growth and agglomeration and subsequently, reduction in the effective surface area of tin dioxide powders. Therefore, it is critical to optimize calcination temperature and time for obtaining high surface area tin dioxide powders via homogeneous precipitation.

## 4. Conclusions

Homogeneous precipitation was successfully utilized to synthesize nanosized $SnO_2$ ceramic particles. Decomposition of urea at ∼90 °C resulted in precipitation of hydrous tin dioxide from 0.001 to 1 M $SnCl_4$-urea aqueous solutions. It has been shown that initial concentration has a significant effect on crystallite size. As initial concentration increased, crystallite size of the calcined tin dioxide increased. Tin dioxide ceramic particles as small as a few nanometers were obtained by homogeneous precipitation. However, crystal growth and agglomeration and subsequently, reduction in the effective surface area of tin dioxide powders occurred during calcination.

## Acknowledgements

This research program was funded by Anadolu University (A.U.) Scientific Research Projects Commission (Project no. 010263) and Turkish State Planning Organization (DPT2003K120170). The authors wish to thank S. Alkoy and A.Y. Oral of Gebze Institute of Technology for SEM data, E. Yorukogullari for BET data and A.U. Plant and Scientific Research Center for FTIR data.

## References

[1] L. Chou, Y. Cai, B. Zhang, J. Niu, S. Ji, S. Li, Infuence of $SnO_2$-doped W-Mn/$SiO_2$ for oxidative conversion of methane to high hydrocarbons at elevated pressure, Appl. Catal. A: Gen. 238 (2003) 185–191.
[2] P.T. Wierzchowski, L.W. Zatorski, Kinetics of catalytic oxidation of carbonmonoxide and methane combustion over alumina supported $Ga_2O_3$, $SnO_2$ or $V_2O_5$, Appl. Catal. B: Environ. 1352 (2003) 1–13.
[3] A.J. Moulson, J.M. Herbert, Electroceramics, Chapman & Hall, New York, 1990.
[4] Y. Shimizu, M. Egashira, Basic aspects and challenges of semiconductor gas sensors, MRS Bull. 24 (6) (1999) 18–24.
[5] M. Kojima, F. Takahashi, K. Kinoshita, T. Nishibe, Ichidate M transparent furnace made of heat mirror, Thin Solid Films 392 (2001) 349–354.
[6] C.M. Lampert, Heat mirror coatings for energy conserving windows, Solar Energy Mater. 6 (1) (1981) 1–41.
[7] J.F. Wang, Y.J. Wang, W.B. Su, H.C. Chen, W.X. Wang, Novel (Zn,Nb)-doped $SnO_2$ varistors, Mater. Sci. Eng. B96 (2002) 8–13.
[8] M.R.C. Santos, P.R. Bueno, E. Longo, J.A. Varela, Effect of oxidizing and reducing atmospheres on the electrical properties of dense $SnO_2$ based varistors, J. Eur. Ceram. Soc. 21 (2) (2001) 161–167.
[9] T.E. Moustafid, H. Cachet, B. Tribollet, D. Festy, Modified transparent $SnO_2$ electrodes as efficient and stable cathodes for oxygen reduction, Electrochim. Acta 47 (8) (2002) 1209–1215.
[10] M. Okuya, S. Kaneko, K. Hiroshima, I. Yaggi, K. Murakami, Low temperature deposition of $SnO_2$ thin films as transparent electrodes by spray pyrolysis of tetra-*n*-butyltin(IV), J. Eur. Ceram. Soc. 21 (10–11) (2001) 2099–2102.
[11] T.W. Kim, D.U. Lee, D.C. Choo, J.H. Kim, H.J. Kim, J.H. Jeong, M. Jung, J.H. Bahang, H.L. Park, Y.S. Yoon, J.Y. Kim, Optical parameters in $SnO_2$ nanocrystalline textured films grown on p-lnSb (1 1 1) substrates, J. Phys. Chem. Solids 63 (2002) 881–885.
[12] K.C. Song, Y. Kang, Preparation of high surface area tin oxide powder by a homogeneous precipitation method, Mater. Lett. 42 (2000) 283–289.
[13] N. Nitta, S. Otani, M. Haradome, Temperature dependence of resistivity of Sn-based gas sensors exposed to CO, $H_2$ and $C_3H_8$ gases, J. Electron. Mater. 9 (4) (1980) 727–743.
[14] F. Li, L. Chen, Z. Chen, J. Xu, J. Zhu, X. Xin, Two-step solid state synthesis of tin oxide and its gas-sensing property, Mater. Chem. Phys. 73 (2002) 335–338.
[15] K.C. Song, J.H. Kim, Preparation of nanosize tin oxide particles from water-in-oil microemulsions, J. Colloid Interf. Sci. 212 (1999) 193–196.
[16] G. Zhang, M. Liu, Preparation of nanostructured tin oxide using a sol–gel process based on tin tatrachloride and ethylene glycol, J. Mater. Sci. 34 (1999) 3213–3321.
[17] J.H. Lee, S.J. Park, Preparation of spherical $SnO_2$ powders by ultrasonic spray pyrolysis, J. Am. Ceram. Soc. 76 (1993) 777–780, 9.
[18] M. Bhagwat, P. Shah, V. Ramaswamy, Synthesis of nanocrystalline $SnO_2$ powder by amorphous citrate route, Mater. Lett. 57 (2003) 1604–1611.
[19] N.S. Baik, G. Sakai, N. Miura, N. Yamazoe, Preparation of stabilized nanosized tin oxide particles by hydrothermal treatment, J. Am. Ceram. Soc. 83 (2000) 2983–2987.
[20] R.E. Riman, The chemical synthesis of ceramic powders, in: R.J. Pugh, L. Bergström (Eds.), Surface and Colloid Chemistry in Advanced Ceramics Processing, Marcel Dekker Inc., 1994.
[21] L. Gordon, M.L. Salutsky, H.H. Willard, Precipitation from Homogeneous Solution, John Wiley & Sons Inc., Chapman & Hall Limited, New York, London, 1959.
[22] H.H. Willard, N.K. Tang, A study of the precipitation of aluminum basic sulfate by urea, J. Am. Chem. Soc. 59 (1937) 1190.
[23] L. Gordon, The precipitation of hydrous oxides of tin and thorium from homogeneous solution by the hydrolysis of non-ionizable compounds, Ph.D. dissertation, The University of Michigan, 1947.
[24] O. Acarbas, E. Suvaci, A. Dogan, Synthesis of nanosized tin oxide particles by homogeneous precipitation, Key Eng. Mater. 264–268 (2004) 1205–1208.
[25] D.A. Popescu, F.B. Verduraz, Infrared studies on $SnO_2$ and Pd/$SnO_2$, Catalysis Today 70 (2001) 139–154.
[26] S. Kato, H. Unuma, T. Ota, M. Takahashi, Homogeneous precipitation of hydrous tin oxide powders at room temperature using enzymatically induced gluconic acid as a precipitant, J. Am. Ceram. Soc. 83 (4) (2000) 986–988.
[27] B.D. Cullity, Elements of X-ray Diffraction, Addison-Wesley Pub. Co., Reading, MA, 1978.
[28] A.E. Nielsen, Kinetics of Precipitation, Pergamon, Oxford, 1969.
[29] G.A. Rossetti Jr., D.J. Watson, R.E. Newnham, J.H. Adair, Kinetics of the hydrothermal crystallization of the perovskite lead titanate, J. Crystal Growth 116 (1992) 251–259.
[30] O. Ozer, E. Suvaci, A. Dogan, J. Eur. Ceram. Soc., submitted for publication.